Available online at www.sciencedirect.com

SciVerse ScienceDirect

Ceramics International 38 (2012) 6525–6529

CERAMICS INTERNATIONAL

www.elsevier.com/locate/ceramint

Phase transition and negative thermal expansion properties of $Sc_{2-x}Cr_xMo_3O_{12}$

M.M. Wu[a,*], J. Peng[b], S.B. Han[a], Z.B. Hu[c], Y.T. Liu[a], D.F. Chen[a]

[a]China Institute of Atomic Energy, Beijing 102413, China
[b]Experimental Physics Center, Institute of High Energy Physics, CAS, Beijing 100049, China
[c]College of Materials and Photoelectric Technology, Graduate University of Chinese Academy of Sciences, Beijing 100049, China

Received 8 April 2012; received in revised form 11 May 2012; accepted 11 May 2012
Available online 17 May 2012

Abstract

The crystal structure, phase transition and thermal expansion behaviors of solid solutions $Sc_{2-x}Cr_xMo_3O_{12}$ ($0 \le x \le 2$) were investigated using X-ray diffraction (XRD) and differential scanning calorimetry (DSC). At room temperature, samples with $x \le 0.7$ and $x \ge 0.8$ crystallize in orthorhombic and monoclinic structures, respectively. DSC result indicates that the phase transition of $Sc_{0.5}Cr_{1.5}Mo_3O_{12}$ from monoclinic to orthorhombic structure occurs at 203.66 °C. The linear thermal expansion coefficient of orthorhombic phases varies from $-2.334 \times 10^{-6}\,°C^{-1}$ to $0.993 \times 10^{-6}\,°C^{-1}$ when x increases from 0.0 to 1.5. The near-zero linear thermal expansion coefficients of $-0.512 \times 10^{-6}\,°C^{-1}$ and $-0.466 \times 10^{-6}\,°C^{-1}$ are observed for compounds with $x=0.5$ and 0.7, respectively.

Keywords: C. Thermal expansion; Molybdates; X-ray diffraction

1. Introduction

Materials with negative thermal expansion (NTE) are of considerable interest. Combining them with positive thermal expansion materials could produce composite materials with adjustable thermal expansion coefficients. Controllable thermal expansion composites are widely used in electrical, optical, and high-temperature devices [1,2]. NTE behavior has been observed in many tungstates and molybdates with the general formula of $A_2M_3O_{12}$, where A is a trivalent ion ranging from Al to Dy. Thus, it is possible to modify the thermal expansion coefficient of $A_2M_3O_{12}$ through partial chemical substitution of the A^{3+} cation by another trivalent cation [3–10].

Existing literatures reported that $Sc_2Mo_3O_{12}$ and $Cr_2Mo_3O_{12}$ [11,12] crystallize in monoclinic structure ($P2_1/a$) at low temperature and transform to orthorhombic structure ($Pnca$) upon heating. Both compounds with monoclinic structure exhibit positive thermal expansion. Orthorhombic $Sc_2Mo_3O_{12}$ exhibits NTE at the temperature range of −93 °C to 27 °C and a linear thermal expansion coefficient α_l ($\alpha_l=\alpha_v/3$) of $-2.1 \times 10^{-6}\,°C^{-1}$, whereas orthorhombic $Cr_2Mo_3O_{12}$ demonstrates positive thermal expansion at the temperature range of 450–800 °C and an α_l value of $0.708 \times 10^{-6}\,°C^{-1}$. Therefore, solid solutions $Sc_{2-x}Cr_xMo_3O_{12}$ with controllable thermal expansion could be obtained by cautiously adjusting the Sc^{3+}/Cr^{3+} ratio.

In this work, a series of $Sc_{2-x}Cr_xMo_3O_{12}$ ($0 \le x \le 2$) ceramics were successfully prepared. The effects of substituted Cr content on the crystal structure, phase transition and thermal expansion were studied.

2. Experiments

All $Sc_{2-x}Cr_xMo_3O_{12}$ ($0 \le x \le 2$) samples were prepared through the solid-state method. Stoichiometric amounts of Sc_2O_3 (purity 99.95%), Cr_2O_3 (purity 99.9%), and MoO_3 (purity ≥ 99.0%) were weighted and fully ground together in an agate mortar, and then calcined at 750–850 °C for 48 h with intermittent regrinding, finally cooling to room temperature in the furnace. Phase identifications of the

*Corresponding author. Tel.: +86 10 69358741; fax: +86 10 69357787.
E-mail address: mmwu@ciae.ac.cn (M.M. Wu).

0272-8842/$36.00 © 2012 Elsevier Ltd and Techna Group S.r.l. All rights reserved.
http://dx.doi.org/10.1016/j.ceramint.2012.05.033

$Sc_{2-x}Cr_xMo_3O_{12}$ compounds were performed through XRD on a MSAL-XD2 diffractometer using Cu K_α radiation at Laboratory of Inorganic Materials of Graduate University of Chinese Academy of Sciences.

The thermal expansion behavior of $Sc_{2-x}Cr_xMo_3O_{12}$ was investigated via PAN X' Pert PRO MPD XRD with X' Celerator as detector and Anton Parr high temperature attachment at Beijing Normal University. High-temperature XRD data for $Sc_{2-x}Cr_xMo_3O_{12}$ ($x=0.0$, 0.5, 0.7 and 1.5) were recorded at 25, 150, 250, 400, 550, 700 and 800 °C in the 2θ range of 10–80°. The sample was heated to the desired temperature on a platinum strip at a rate of 30 °C/min and kept for 5 min for equilibration before XRD data were collected. The positions of the reflections and lattice parameters were calculated through the least-squares method using the software FullProf Suite 2005 [13]. The phase transition temperature of $Sc_{0.5}Cr_{1.5}Mo_3O_{12}$ was detected through DSC using TA instruments Q100 in nitrogen atmosphere at a heating temperature range of 25–400 °C and a rate of 10 °C/min at Peking University.

3. Results and discussion

3.1. XRD analysis and phase transition

Fig. 1 shows the XRD patterns of the $Sc_{2-x}Cr_xMo_3O_{12}$ ($0 \le x \le 2$) samples at room temperature. The Rietveld method was employed to analyze the diffraction patterns. The atomic parameters for the monoclinic and orthorhombic structure refinement were obtained from those reported for $Fe_2Mo_3O_{12}$ [14] and $Sc_2Mo_3O_{12}$ [11], respectively. All samples appear to be single phase from the XRD refinement, and no detectable impurity phase is present. Sc^{3+} (0.73 Å) and Cr^{3+} (0.63 Å) can be substituted in the whole composition range mutually because of the relatively small difference in their radii. Samples with $x \le 0.7$ have $Sc_2Mo_3O_{12}$-type orthorhombic structures (*P*nca), whereas those with $x \ge 0.8$ exhibit $Cr_2Mo_3O_{12}$-type monoclinic structures ($P2_1/a$). The difference in characteristic diffraction peak between monoclinic and orthorhombic structures is shown in Fig. 1 (as indicated by "*M*"). The lattice parameter dependence on the Cr content, derived from the Rietveld refinement, is shown in Fig. 2. It can be seen that cell parameters *a*, *b*, *c* and volume *V* for monoclinic and orthorhombic $Sc_{2-x}Cr_xMo_3O_{12}$ decrease linearly as Cr content increases. This result can be attributed to the smaller ionic radius of Cr^{3+} than Sc^{3+}. The linear dependence of lattice parameters on Cr content is in good agreement with the Vegard's law, which again proves the successful preparation of the solid solutions $Sc_{2-x}Cr_xMo_3O_{12}$ [15,16].

Most $A_2Mo_3O_{12}$ compounds have been reported to demonstrate phase transition from monoclinic to orthorhombic at a higher temperature [7,17]. The transition temperatures for $Sc_2Mo_3O_{12}$ and $Cr_2Mo_3O_{12}$ are reported to be −95 °C and 401 °C, respectively. In the present study, the transition temperature of $Sc_{0.5}Cr_{1.5}Mo_3O_{12}$ detected via DSC is 203.66 °C (Fig. 3). The partial

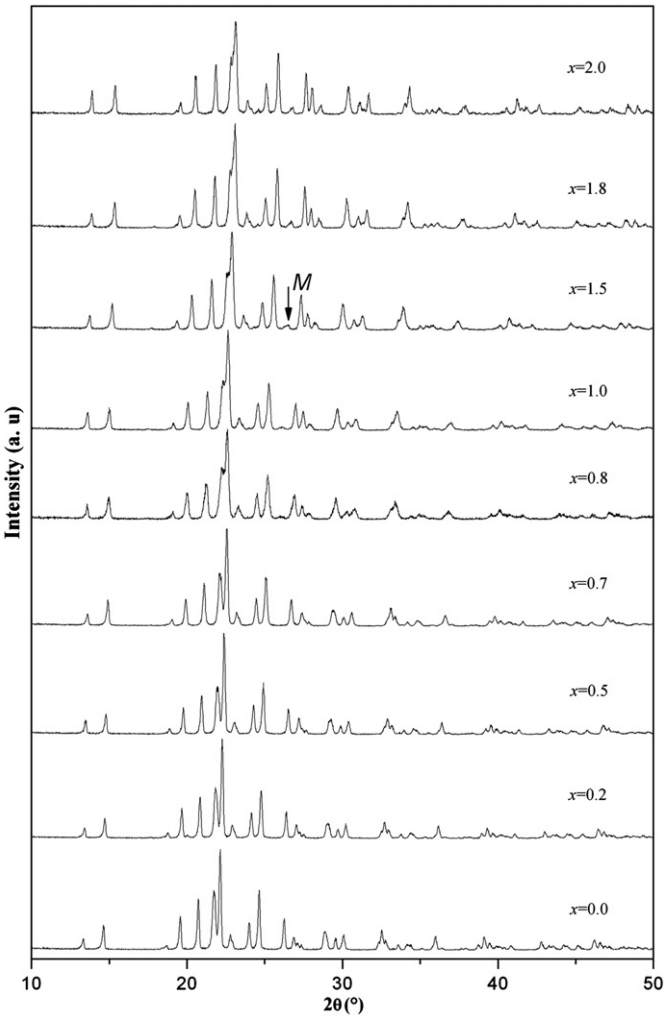

Fig. 1. XRD patterns of $Sc_{2-x}Cr_xMo_3O_{12}$ collected at room temperature.

substitution of Sc^{3+} for Cr^{3+} notably promotes the phase transition from monoclinic to orthorhombic structure. Previous studies suggested that a correlation exists between the phase transition temperature and the electronegativity of A^{3+} cation in the $A_2Mo_3O_{12}$ family [7,18]. As the electronegativity of the A^{3+} cation decreases, the transition temperature decreases. The electronegativity of Sc^{3+} (1.36) is less than that of Cr^{3+} (1.66). Hence, the transition temperature of $Sc_{2-x}Cr_xMo_3O_{12}$ is at a lower temperature with decreasing Cr content, and when $x \le 0.7$, the samples exhibit orthorhombic structure at room temperature.

3.2. Thermal expansion property

The thermal expansion properties of $Sc_{2-x}Cr_xMo_3O_{12}$ ($x=0.0$, 0.5, 0.7 and 1.5) were investigated through high-temperature XRD. Samples with $x=0.0$, 0.5 and 0.7 maintain an orthorhombic structure in the tested temperature range. Sample $Sc_{0.5}Cr_{1.5}Mo_3O_{12}$ exhibits monoclinic structure at and below 150 °C, and transforms to orthorhombic structure above 250 °C. All known monoclinic $A_2Mo_3O_{12}$ compounds show positive thermal expansion.

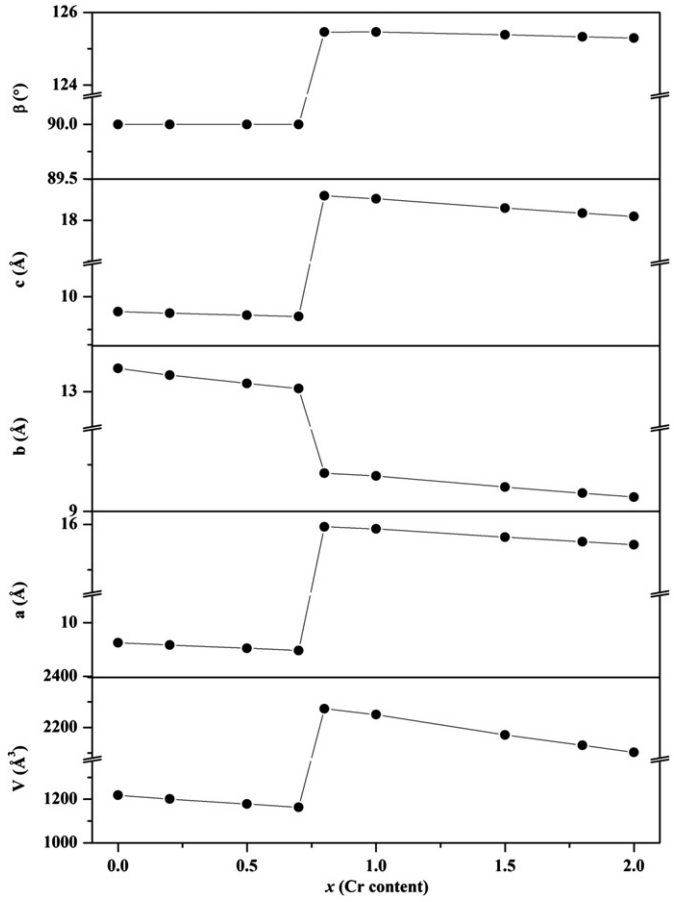

Fig. 2. Cell parameters of $Sc_{2-x}Cr_xMo_3O_{12}$ with different Cr content at room temperature.

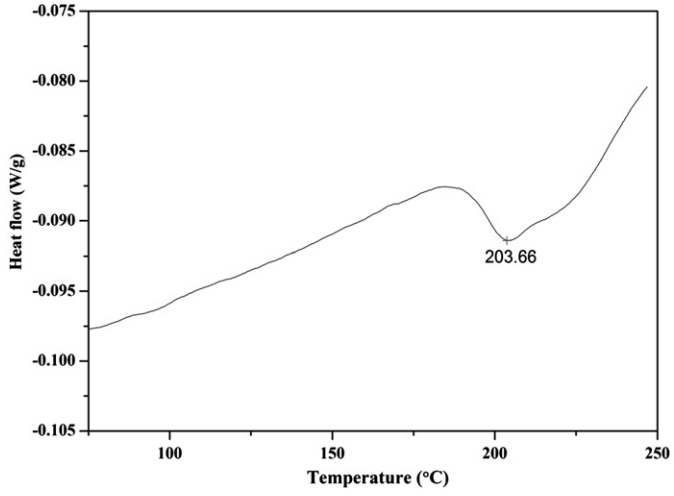

Fig. 3. DSC curve of $Sc_{0.5}Cr_{1.5}Mo_3O_{12}$.

In the present study, the cell parameters a, b and c of monoclinic $Sc_{0.5}Cr_{1.5}Mo_3O_{12}$ increase as temperature increases from 25 °C to 150 °C (Table 1). As a result, the unit cell volume expands significantly.

The variation of cell parameters a, b, c and volume V with temperature of all orthorhombic samples is shown in Fig. 4. As shown in Fig. 4, the a- and c-axes show contraction upon heating, whereas an increase can be observed in the b-axis. The different contraction or expansion coefficients of the three axes lead to their different thermal expansion properties. The α_l values of $Sc_{2-x}Cr_xMo_3O_{12}$ (x=0.0, 0.5, 0.7 and 1.5) are -2.334×10^{-6}, -0.512×10^{-6}, -0.466×10^{-6} and 0.993×10^{-6} °C^{-1}, respectively. As detected through neutron diffraction, the reported α_l value of $Sc_2Mo_3O_{12}$ is -2.1×10^{-6} °C^{-1} between −93 °C and 27 °C. This value is very similar to our result. Table 2 illustrates the axial and linear coefficients of thermal expansion for $Sc_{2-x}Cr_xMo_3O_{12}$ (x=0.0, 0.5, 0.7 and 1.5). As shown in Table 2, α_a, α_b and α_c increase with increasing Cr content, and α_l increases from negative to positive as a result.

Table 1
Cell parameters of $Sc_{0.5}Cr_{1.5}Mo_3O_{12}$ at 25 °C and 150 °C.

	a (Å)	b (Å)	c (Å)	β (°)	V (Å^3)
25 °C	15.723(1)	9.2591(4)	18.292(1)	125.401(2)	2170.6(2)
150 °C	15.751(1)	9.2723(4)	18.332(1)	125.470(3)	2180.5(2)

Orthorhombic and monoclinic structures of $A_2Mo_3O_{12}$ are very similar, both consisting of the corner-sharing network of AO6 octahedra and MoO4 tetrahedra [9]. AO6 octahedra share all six corners with MoO4 tetrahedra, and MoO4 tetrahedra share corners with AO6 octahedra. This sharing leads to the two-fold coordination of oxygen, which is believed to be an essential feature for NTE. However, only orthorhombic compounds may exhibit NTE behavior, the mechanism of which is attributed to the rocking motion of polyhedra related to the transverse vibrations of two-fold coordinated oxygen [2,17]. This transverse vibrational motion of A–O–Mo draws A and Mo atoms closer together and result in the overall lattice shrinkage. Fig. 5 shows the average Sc(Cr)–Mo non-bond distance in $Sc_{2-x}Cr_xMo_3O_{12}$ (x=0.0, 0.7 and 1.5) with rising temperature. The average Sc(Cr)–Mo distance in $Sc_{2-x}Cr_xMo_3O_{12}$ (x=0.0 and 0.7) shows contraction with increasing temperature. This result is in accordance with the thermal expansion property. However, the Sc(Cr)–Mo distance in $Sc_{05}Cr_{1.5}Mo_3O_{12}$ increases upon heating, which indicates that another factor affects the thermal expansion behavior.

The rocking motion of polyhedra necessary for NTE cannot occur without some changes in the shape of the polyhedra. The magnitude of NTE coefficient increases as the ionic radius of the A^{3+} ion increases. The oxygen–oxygen repulsive interaction decreases in AO6 polyhedra with larger central cations, making slight distortions easier to occur, and therefore enhancing NTE behavior [19]. In the case of orthorhombic $Sc_{05}Cr_{1.5}Mo_3O_{12}$, the shape change in Sc(Cr)O6 octahedral is gradually attenuated with strong oxygen–oxygen repulsion, thus giving rise to its positive thermal expansion. The results suggest that the thermal expansion coefficient of ceramic $Sc_{2-x}Cr_xMo_3O_{12}$

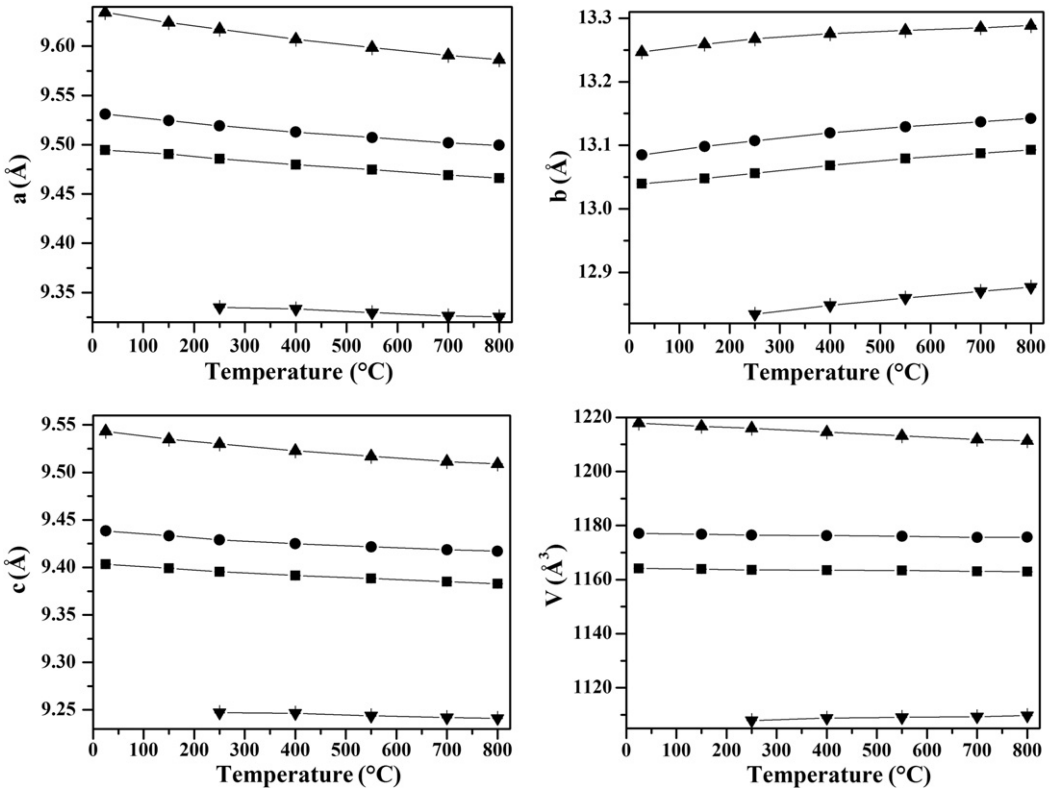

Fig. 4. Lattice parameters as a function of temperature for orthorhombic $Sc_{2-x}Cr_xMo_3O_{12}$ (x=0.0 (▲), 0.5 (●), 0.7 (■) and 1.5 (▼)).

Table 2
Axial and linear thermal expansion coefficients of $Sc_{2-x}Cr_xMo_3O_{12}$.

Compound	$\alpha_a(\times 10^{-6}\,^{\circ}C^{-1})$	$\alpha_b(\times 10^{-6\circ}\,C^{-1})$	$\alpha_c(\times 10^{-6}\,^{\circ}C^{-1})$	$\alpha_l(\times 10^{-6}\,^{\circ}C^{-1})$
x=0.0(25–800 °C)	−6.407	4.070	−4.652	−2.334
x=0.5(25–800 °C)	−4.288	5.680	−2.908	−0.512
x=0.7(25–800 °C)	−3.851	5.267	−2.790	−0.466
x=1.5(250–800 °C)	−1.883	6.023	−1.158	0.993

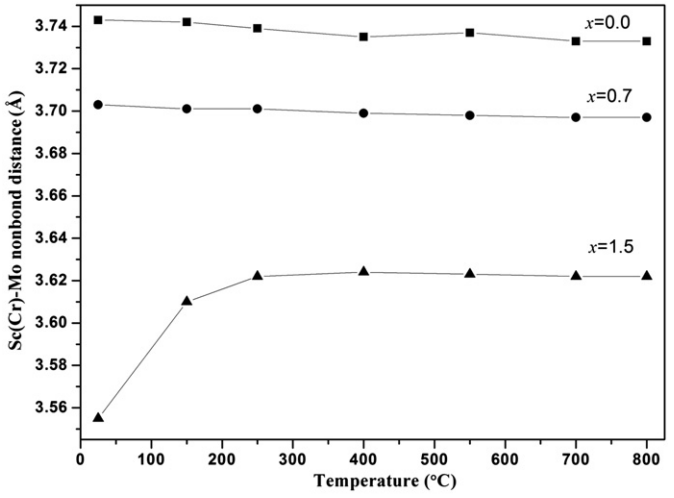

Fig. 5. Selected average Sc(Cr)–Mo non-bond distance with increasing temperature.

can be easily controlled from negative to positive by adjusting the Sc/Cr ratio.

4. Conclusions

Single-phased $Sc_{2-x}Cr_xMo_3O_{12}$ $(0 \le x \le 2)$ samples were prepared. The relationship between the cell parameters and the size of A^{3+} cation follows the Vegard's law for monoclinic and orthorhombic structures. The transition temperature increases with the increasing electronegativity value of A^{3+} cation.

The thermal expansion coefficients for the orthorhombic phase could be controlled by adjusting the Sc/Cr ratio. With increasing Cr content, the thermal expansion behavior of $Sc_{2-x}Cr_xMo_3O_{12}$ varies from negative to positive. Near-zero thermal expansion is observed when x=0.5 and 0.7, with α_l being -0.512×10^{-6} and $-0.466-10^{-6}\,^{\circ}C^{-1}$, respectively. As the size of A^{3+} decreases, the oxygen–oxygen repulsion

increases within the polyhedra, and the distortion necessary for NTE become difficult, leading to positive thermal expansion coefficient.

Acknowledgment

Financial supports from National Natural Science Foundation of China (NSFC) (Grant no. 10905095, 11105159) and 973 programs (2010CB833101) are greatly appreciated.

References

[1] J.S.O. Evans, T.A. Mary, A.W. Sleight, Negative thermal expansion materials, Physica B 241 (1997) 311–316.
[2] J.S.O. Evans, Negative thermal expansion, Journal of the Chemical Society Dalton Transactions (1999) 3317–3326.
[3] T.A. Mary, A.W. Sleight, Bulk thermal expansion for tungstate and molybdates of the type $A_2M_3O_{12}$, Journal of Materials Research 14 (3) (1999) 912–915.
[4] P.M. Forster, A. Yokochi, A.W. Sleight, Enhanced negative thermal expansion in $Lu_2W_3O_{12}$, Journal of Solid State Chemistry 140 (1998) 157–158.
[5] S. Sumithra, A.M. Umaji, Negative thermal expansion in rare earth molybdates, Solid State Sciences 8 (2006) 1453–1458.
[6] A.W. Sleight, Isotropic negative thermal expansion, Annual Review of Materials Science 28 (1998) 29–43.
[7] J.S.O. Evans, T.A. Mary, A.W. Sleight, Negative thermal expansion in a large molybdate and tungstate family, Journal of Solid State Chemistry 133 (1997) 580–583.
[8] Y.Z. Cheng, M.M. Wu, J. Peng, X.L. Xiao, Z.X. Li, Z.B. Hu, R. Kiyanagi, J.S. Fieramosca, S. Short, J. Jorgensen, Structures, thermal expansion properties and phase transitions of $Er_xFe_{2-x}(MoO_4)_3$ ($0.0 \le x \le 2.0$), Solid State Sciences 9 (8) (2007) 693–698.
[9] M. Ari, P.M. Jardim, B.A. Marinkovic, F. Rizzo, F.F. Ferreira, Thermal expansion of $Cr_{2x}Fe_{2-2x}Mo_3O_{12}$, $Al_{2x}Fe_{2-2x}Mo_3O_{12}$ and $Al_{2x}Cr_{2-2x}Mo_3O_{12}$ solid solutions, Journal of Solid State Chemistry 181 (2008) 1472–1479.
[10] H.F Liu, W. Zhang, Z.P. Zhang, X.B Chen, Synthesis and negative thermal expansion properties of solid solutions $Yb_{2-x}La_xW_3O_{12}$ ($0 \le x \le 2$), Ceramics International 38 (2012) 2951–2956.
[11] J.S.O. Evans, T.A. Mary, Structural phase transitions and negative thermal expansion in $Sc_2(MoO_4)_3$, International Journal of Inorganic Materials 2 (2000) 143–151.
[12] M.M. Wu, X.L. Xiao, Z.B. Hu, Y.T. Liu, D.F. Chen, Controllable thermal expansion and phase transition in $Yb_{2-x}Cr_xMo_3O_{12}$, Solid State Sciences 11 (2) (2009) 325–329.
[13] J. Rodriguez-Carjaval, in: J. Rodriguez-Carjaval (Ed.), An Introduction to the Program FULLPROF2000 (Version July 2005), Laboratoire Leon Brillouin (CEACNRS), France, 2005.
[14] H.Y. Chen, The crystal structure and twinning behavior of ferric molybdate, $Fe_2(MoO_4)_3$, Materials Research Bulletin 14 (1979) 1583–1590.
[15] M.J. Lambregts, S. Frank, Application of Vegard's law to mixed cation sodalites: a simple method for determining the stoichiometry, Talanta 62 (2004) 627–630.
[16] V.A. Lubarda, On the effective lattice parameter of binary alloys, Mechanics of Materials 35 (2003) 53–68.
[17] A.W. Sleight, L.J. Brixner, A new ferroelastic transition in some $A_2(MO_4)_3$ molybdates and tungstates, Journal of Solid State Chemistry 7 (1973) 172–174.
[18] B.A. Marinkovic, P.M. Jardim, R.R. deAvillez, F. Rizzo, Negative thermal expansion in $Y_2Mo_3O_{12}$, Solid State Sciences 7 (2005) 1377–1383.
[19] B.A. Marinkovic, M. Ari, R.R. deAvillez, F. Rizzo, F.F Ferreira, K.J. Miller, M.B Johnson, M.A. White, Correlation between AO6 polyhedral distortion and negative thermal expansion in orthorhombic $Y_2Mo_3O_{12}$ and related materials, Chemistry of Materials 21 (2009) 2886–2894.